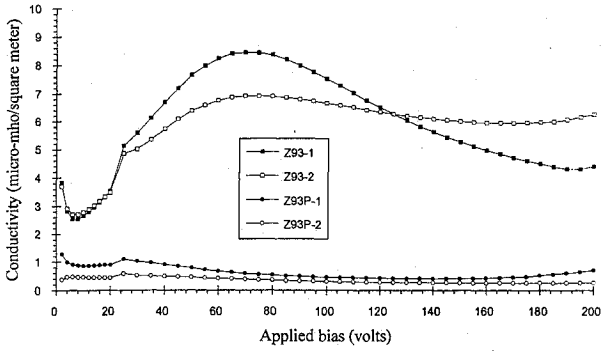

Fig. 2 Electron conductivity vs applied bias.

stant. Figure 2 supports the same conclusion for electron collection, i.e., a constant conductivity.

Conductivity for Z93 shows a more pronounced dependence on voltage for both electron and ion conductivity. While these curves may be used for more accurate estimates, one can say that the conductivity over the 50- to 150 V range is approximately a factor of 10 larger than for Z93P.

In estimating the overall error in our reported results, recall first that data were taken in five run sets. Data from metal samples shows typical standard errors in the 1 to 2% range, indicating stable, reproducible plasma conditions. Data from the coating samples, however, show much larger errors, generally 20 to 30% in magnitude. These relatively large errors are not, however, randomly distributed, but indicate a systematic effect in the experiment. Since the runs were not all taken at the same time, comparison of the time history of the runs with raw data indicates that the history of the sample in the 15 to 20 min previous to a run is critical. Specifically, if two runs are taken with no delay between them, the second differs from the first by as much as a factor of 2. If, however, 15 to 20 min is allowed to pass, the second run reproduces the first to within a few percent. Since the samples are exposed to active plasma at all times, we do not believe this to be a residual charging effect. Apparently, the application of high voltage to this material temporarily alters its bulk properties in a way that requires a significant time to relax. The mechanism is unknown and will be the subject of future research relating to this family of coatings. This effect, along with the 2- to 3-V error in our voltage scale discussed above, leads us to believe that our final mean conductivities are conservatively accurate to no better than a factor of two.

Conclusions

The plasma conductivity of Z93 and Z93P thermal control coatings was measured directly in a space simulation chamber. For Z93P, which is assumed to be the baseline formulation for all future applications, the conductivity was found to be a nearly constant 0.5 μS/m^2. For Z93, the previous formulation, conductivity was approximately an order of magnitude larger and showed a somewhat more pronounced dependence on voltage. As is noted above, there are small differences in the composition of the binder between the two coatings, which presumably account for the measured differences in conductivity. These results are being incorporated into modeling for ISSA. Preliminary results[6] indicate that the conductivity we report here is two orders of magnitude too small to affect the current balance and floating potential significantly. Our results will be used to advocate the development of coatings with mechanical, thermal, and optical properties similar to Z93P but with an electrical conductivity that can be tailored to the application

Acknowledgments

All coating samples were prepared for NASA by Yoshiro Harada, IIT Research Institute, Chicago. The author thanks Joyce Dever, NASA Lewis, who has been a major participant in the requalification program for zinc oxide coatings and who provided considerable encouragement and support for this work.

References

[1]Ferguson, D. C., Snyder, D. B., and Carruth, R., "Findings of the Joint Workshop on Evaluation of Impacts of Space Station Freedom Grounding Configurations," NASA TM-103717, Oct. 1990.

[2]Brewer, D., private communication, Space Station Freedom Project Office, Reston, VA, Oct. 1991.

[3]Stoyack, J. E., "Z93 Reformulation evaluation," Design Information Release 3-47300H/3DIR-016, Loral Vought Systems Corp., Jan. 1993.

[4]Hillard, G. B., "Plasma Current Collection of Z93 Thermal Control Coating as Measured in the Lewis Research Center's Plasma Interaction Facility," NASA TM-106132, April 1993.

[5]Hillard, G. B., "Experimental Measurement of the Plasma Conductivity of Z93 and Z93P Thermal Control Paint," NASA TM-106284, Sept. 1993.

[6]Purvis, C. K., "Environments Workbench Analysis of on-Orbit Floating Potentials of Space Station Freedom," Paper 93IEC-278AP-9, Aug. 1993.

Launch Strategy Using Ground-Based Mass Drivers

Richard B. Peterson*
Oregon State University, Corvallis, Oregon 97331

I. Introduction

THERE is current interest in developing a ground-based mass driver for accelerating payloads to near-orbital velocities.[1-3] This idea would exclude the possibility of delivering personnel, but supplies that could withstand high acceleration could be launched inexpensively several times a day. The idea presented here would make use of high-repetition drivers to accelerate small packages of matter. This would create a "fountain" to push a larger vehicle through the atmosphere and into space. The packages leaving the mass driver are envisioned as being slugs of solid material that can survive transit through the atmosphere yet disintegrate upon impact with a pusher plate at the aft of the accelerating vehicle. The repetition rate would be between 10 and 100 per second, and the relative velocity between the slugs and the vehicle would be held constant. The high repetition rate of the slug stream might make it easier for the following slugs to arrive at the vehicle. Note that this concept has been suggested before for powering interstellar missions,[4,5] where the benefits of a vacuum are present but extremely long distances are involved.

II. Momentum Transfer to Vehicle

Two components make up the propulsive effect when the slugs arrive at the vehicle. The first is the momentum transfer from collisions. This could take the form of each slug disintegrating upon impact with a flat plate, so that momentum is transferred in the amount of $m_s V_r$, where m_s is the mass of the slug and V_r is the relative velocity between the slug and the vehicle. Higher momentum transfer would result from a concave pusher plate. A second possible propulsive effect could arise from the kinetic or chemical energy that is delivered with the slugs. Only the case of momentum transfer will be considered here, and we further simplify the analysis by ignoring two effects, namely drag forces and Earth's gravity field. Both would be important in a detailed analysis, but the purpose of this write-up is to arrive at order-of-magnitude values for the major parameters describing the launch concept.

The required slug mass, relative velocity, and repetition rate can be worked out given the mission specifications. The baseline vehicle will have a mass of 10,000 kg and accelerate at a rate between 19.6 and 69.6 m/s^2 ($3g$ and $7g$). The final velocity will be arbitrarily set

Received Oct. 5, 1992; revision received Nov. 17, 1992; accepted for publication Nov. 17, 1992.

*Professor, Department of Mechanical Engineering.

at 70% of orbital velocity, or roughly 5.5 km/s. The force on the vehicle will be,

$$F_v = \phi N m_s V_r \tag{1}$$

where ϕ varies between 1 and 2 depending on whether the slug mass is turned through 90 or 180 deg, and N is the number of slugs arriving at the pusher plate per second. Note that it is convenient to assume a constant relative velocity between the slugs and the vehicle. This, however, may present difficulties in timing the acceleration of the slugs with respect to their eventual arrival at the vehicle. Using Eq. (1) and Newton's second law, the required slug flow rate is

$$N m_s = \frac{a_v m_v}{\phi_r V_r} \tag{2}$$

where m_v and a_v are the mass and acceleration of the vehicle, respectively. The quantity Nm_s is plotted in Fig. 1 as a function of V_r.

III. Mass-Driver Requirements

The power supplied to the mass driver will increase as the vehicle accelerates, due to ramping of the slug velocity. Starting with the kinetic energy of each slug, we can multiply by the number of slugs per second in order to obtain the power. After appropriate substitutions and rearranging, the mass-driver power becomes

$$P_a = \frac{a_v m_v}{\phi}\left(V_v + \frac{V_r}{2} + \frac{V_v^2}{2V_r}\right) \tag{3}$$

where V_v is the vehicle velocity. Figure 2 shows the power supplied to the mass driver as a function of vehicle velocity for various values of a_v and V_r. The trend shows increasing driver power as the vehicle attains higher speeds, with a maximum in the 1- to 3-GW range. Given the maximum sustainable acceleration of approximately $7g$ for personnel, this gives a maximum power of 2.2 GW for a final velocity of 5.5 km/s and for a relative velocity of 600 m/s. The distance and time needed to accelerate to this velocity are 220 km and 80 s, respectively.

Another important aspect to consider is the efficiency in transmitting the mass-driver energy to the vehicle. The driver power is first integrated between the limits 0 and t to obtain the total energy. This quantity can be divided into the energy acquired by the vehicle during the same time period. Doing this and rearranging yields,

$$\mathrm{EFF} = \phi\left(1 + \frac{V_r}{a_v t} + \frac{a_v t}{3V_r}\right)^{-1} \tag{4}$$

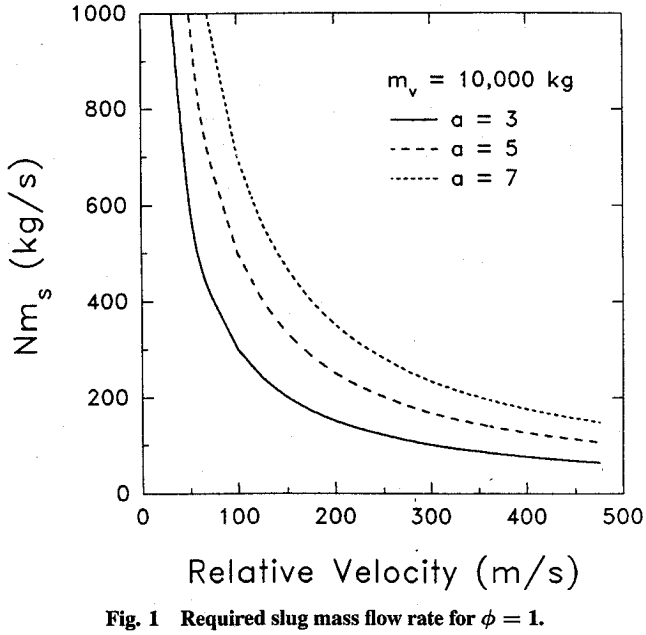

Fig. 1 Required slug mass flow rate for $\phi = 1$.

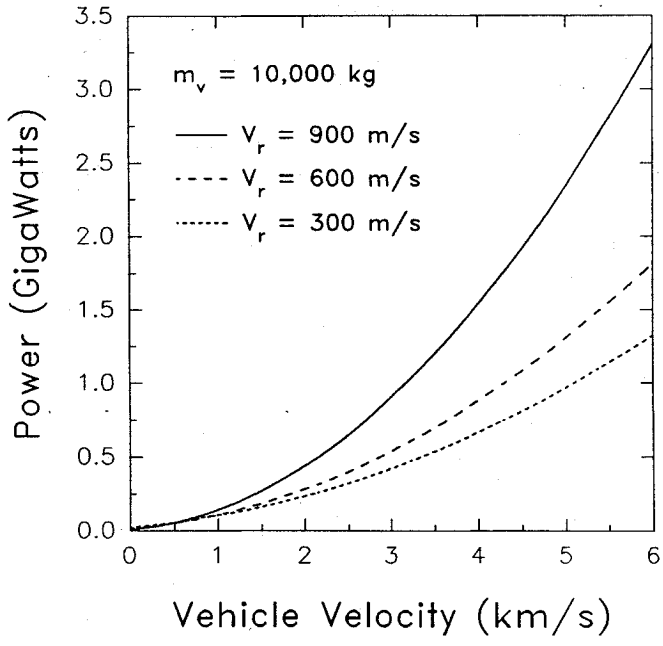

Fig. 2 Mass-driver power requirements for a vehicle acceleration of $5g$ and $\phi = 1$.

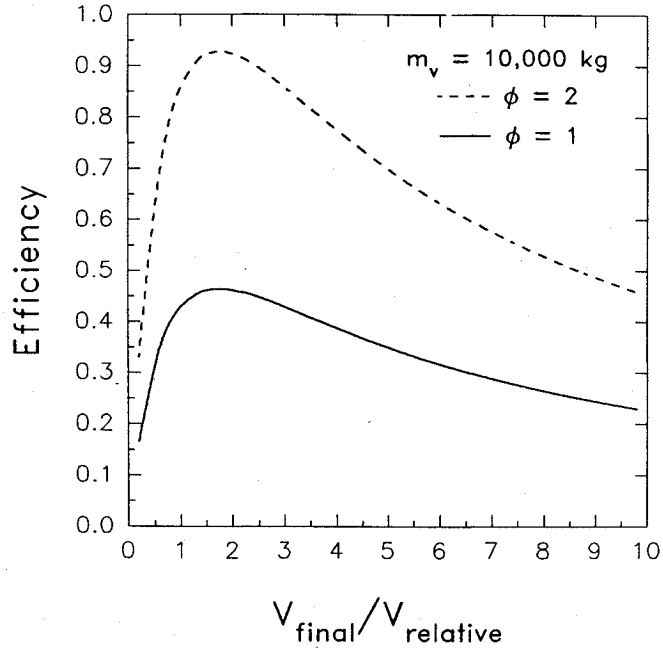

Fig. 3 Energy efficiency of the acceleration process.

A simplification results on substituting V_v for $a_v t$ to obtain

$$\mathrm{EFF} = \phi\left(1 + \frac{\beta}{3} + \frac{1}{\beta}\right)^{-1} \tag{5}$$

where β is equal to V_v/V_r. This expression is plotted in Fig. 3 for two cases of ϕ. A maximum for each curve exists at 1.75, indicating that this value of β would provide the maximum energy transfer to the accelerating vehicle. Unfortunately, achieving orbital velocity in the most efficient way requires a very high relative velocity and brings into doubt whether the pusher plate would survive.

IV. Other Considerations

Besides the mass driver, there are other major constraints to be satisfied before this launch scheme can be considered for use. For example, each slug must leave the mass driver with precisely defined speed and direction to arrive at the pusher plate, which may be

up to 200 km away. Also, wind patterns and the wake region behind each slug will have a major influence on the path of the slugs. At high repetition rates it is anticipated that slug passage through the atmosphere will be beneficially affected. However, for this concept to work the impact diameter at the vehicle must be held to approximately 10 m. Some maneuvering by the vehicle is acceptable for gross changes in the slug stream, but if the slugs arrive with a large random dispersion, the vehicle will not be able to respond to the individual slugs. Further work is needed on this subject.

The final factor considered here is the possibility that either kinetic energy or some form of chemical energy carried by the slugs can be put to use. If the kinetic energy of the arriving mass could be converted directly into thermal energy upon collision, the vapor thus formed could be harnessed to provide propulsive thrust to the ascending vehicle. For example, a relative velocity of 2 km/s represents an enthalpic value of 2 MJ per kilogram of slug. For slug material composed primarily of water, this enthalpic value is approximately the heat of vaporization at standard pressure. If we go one step further, perhaps a monopropellant cryogenically frozen into a solid form would provide a suitable material that would either burn or detonate on impact. With such a configuration, the scheme proposed here begins to look like a chemically driven Orion-type vehicle relying on a ground-based mass driver for propellant delivery. These interesting variations on the basic concept can be seriously considered once the major question on slug passage through the atmosphere has been resolved.

References

[1]Hawke, R. S., Brooks, A. L., Fowler, C. M., and Peterson, D. R., "Electromagnetic Railgun Launchers: Direct Launch Feasibility," *AIAA Journal*, Vol. 20, No. 7, 1982, pp. 978–985.

[2]Wilbur, P. J., Mitchell, C. E., and Shaw, B. D., "The Electrothermal Ramjet," *AIAA Journal*, Vol. 20, No. 6, 1983, pp. 603–610.

[3]Jones, G. R., Swanson, N. J., Madura, D. L., and Bohannon, R. C., "Aerothermodynamic Issues Associated with Rail Gun Launched to Space Projectiles," AIAA Paper 90-1720, June 1990.

[4]Singer, C. E., "Interstellar Propulsion Using a Pellet Stream for Momentum Transfer," *Journal of the British Interplanetary Society*, Vol. 33, No. 3, 1980, pp. 107–115.

[5]Rupp, H. O., "Comments on 'Interstellar Propulsion Using a Pellet Stream for Momentum Transfer' by C. E. Singer," *Journal of the British Interplanetary Society*, Vol. 34, No. 3, 1981, pp. 115–116.

Effect of Transverse Vibration on the Performance of a Heat Pipe

Mark C. Charlton* and W. Jerry Bowman†
Air Force Institute of Technology,
Wright-Patterson Air Force Base, Ohio 45433

Introduction

THE growing number of current and potential applications for heat pipes brings with it an expanding set of environmental conditions under which the heat pipe must function. This research is a step toward evaluating what effect, if any, these environmental conditions have on the capabilities of heat pipes. In particular, this experiment examined how a heat pipe might operate in an environment where it is subjected to vibration.

Received May 28, 1993; presented as Paper 93-2734 at the AIAA 28th Thermophysics Conference, Orlando, FL, July 6–9, 1993; revision received Sept. 25, 1993; accepted for publication Oct. 4, 1993.

*Graduate Student.
†Associate Professor of Aerospace Engineering. Senior Member AIAA.

A literature search revealed that little research has been done on the effects of vibration on heat pipe performance. Deverall[1] reported on an experiment designed to evaluate the effect of vibration on a heat pipe. The conclusion to this report is that "sinusoidal and random vibration, within the spectrum tested, are not detrimental to heat pipe performance." A second work addressing this subject was a report by Richardson et al.[2] They investigated the effect of longitudinal vibration on heat pipe performance. It was reported that the effect is greater at lower frequencies and higher amplitudes. The authors indicated that "the most pressing need is for an investigation providing information on actual maximum heat transfer capability" and that "an investigation should be made of the effect of transverse vibration."

The objective of this research is to determine the effect of transverse vibration on the capillary limit of a heat pipe. To attain this objective, an experimental heat pipe and apparatus were designed and built. The static performance of the pipe was first measured through a series of tests with no vibration input. These tests provided a baseline of maximum heat transport for the pipe over a range of heat pipe operating temperatures. Once this baseline performance was established, tests were run with vibration input perpendicular to the longitudinal axis of the pipe. The results from the vibration test runs were compared to those from the static baseline runs to determine if there was any effect on the maximum heat transport due to transverse vibration.

Experiment Design

The heat pipe used during the experiment was constructed of oxygen-free hard copper. It consisted of a section of pipe 0.3175 m in length to allow for a 0.3048-m total working length after installation of the endcaps, each of which had a total depth of 0.6350 cm. The outside diameter of the pipe was 2.223 cm and the inside diameter was 1.892 cm. The wall thickness was 1.651 mm. It had a condenser section 0.1111 m long, an adiabatic section 0.09210 m long, and an evaporator section 0.1016 m long. Fig. 1 is an illustration of the pipe.

The wick was constructed of 100-mesh copper screen. It had a length of 0.3048 m and a width of .01191 m to allow for two complete wraps of screen. 5.7 g of water were inserted into the heat pipe as the working fluid. All parts were given a final cleaning before assembly, closing, and filling of the pipe. The cleaning and fill process are discussed in detail in Ref. 3.

A flexible tape heater was used to heat the evaporator end of the heat pipe. This heater had a length of 1.829 m and a width of 1.270 cm. The maximum power of the heater was 470 W at 120 V, and it had a power density of 2.015×10^4 W/m^2. With an evaporator section length of only 0.1016 m, the heater was wrapped in layers in order to get sufficient power density to run the experiment. The heater was insulated. This is turn was covered with an aluminum foil adhesive tape to hold the batting together during vibration. The electrical power input to the heater was monitored using a voltmeter and an ammeter.

A coolant control system was required in order to operate the pipe at various temperatures. While the pipe was operating in the heat pipe mode, the pipe operating temperature could be varied by varying the condenser temperature. This was accomplished by changing the coolant flow rate. Normal tap water was used as a coolant and was run through the manifold surrounding the condenser section of the heat pipe. The coolant inlet temperature was not controlled and was determined by the temperature of the water in the building plumbing.

The data acquisition system for this experiment had to be capable of reading and storing vibration frequency and amplitude data, temperature data, heater power data, and coolant flow-rate data. The vibration data were measured using accelerometers. The vibration in the actuator axis direction was the control variable for the experiment, so it was at a known frequency and amplitude. The vibration frequency and amplitude in the other two directions were measured using single-axis accelerometers aligned with these axes and mounted on the vibration fixture. The output from the "off-axis" accelerometers was routed into an oscilloscope for display. The readings for the off-axis vibration amplitudes were taken man-